

Multidimensional HBT correlations in $p\bar{p}$ collisions at $\sqrt{s} = 630 \text{ GeV}$ ¹

H.C. Eggers^a, B. Buschbeck^b and F.J. October^{c,a}

^a *Department of Physics, University of Stellenbosch, 7602 Stellenbosch, South Africa*

^b *Institut für Hochenergiephysik, Nikolsdorfergasse 18, A-1050 Vienna, Austria*

^c *Institute for Maritime Technology, 7995 Simonstown, South Africa*

Abstract

We analyse second moments R_2 of like-sign pion pairs in the two-dimensional (q_L, q_T) and three-dimensional (q_O, q_S, q_L) decompositions of the three-momentum difference. Conventional fit parametrisations such as gaussian, exponential, power-law and Edgeworth fail miserably, while more elaborate ones such as Lévy do well but fail to yield a unique best-fit solution. A two-component model using a hard cut to separate small- and large-scale parts appears possible but not compelling. In all cases, the data exhibits a strong and hitherto unexplained peak at small momentum differences which exceeds current fits.

Classification: 13.85.Hd, 13.87.Fh, 13.85.-t, 25.75.Gz

Keywords: particle correlations, intensity interferometry

The UA1 experiment, having completed data-taking at the CERN SPS in the late eighties, continues to be relevant and interesting. The current concentrated effort at RHIC to quantify and understand ultrarelativistic nuclear collisions relies extensively on comparisons with baseline scenarios constructed from the corresponding “trivial” hadron-hadron sample. Current experimental energies of 200 AGeV at RHIC are still below those available to UA1 by a factor three, so that UA1 results may also provide a window on possible energy dependencies of current investigations.

In this contribution, we provide preliminary results on HBT analysis mainly in terms of the two-dimensional decomposition of the three-momentum difference, defining in the usual way $q_L = |\mathbf{q}_L| = |(\mathbf{q} \cdot \hat{z}) \hat{z}|$, with \hat{z} the beam direction, and $q_T = |\mathbf{q} - \mathbf{q}_L|$. Brief reference is also made to the three-dimensional Bertsch-Pratt case, with similar results and issues arising.

Like-sign (LS) pion pairs from approximately 2.45 million minimum-bias events measured by the UA1 central detector were analysed. This represents a twofold increase in statistics over Ref. [1] and a 15-fold increase compared to earlier UA1 HBT analyses [2, 3, 4]. Standard cuts [1] were applied, including single-track cuts $p_\perp \geq 0.15 \text{ GeV}/c$, $|y| \leq 3$ and, to avoid acceptance problems, $45^\circ \leq |\phi| \leq 135^\circ$. The sample contains an estimated 15% contamination of charged kaons.

The most important among the standard pair cuts is the “ghost cut” which eliminates spurious “split track” LS pairs within a narrow cone but many real LS pairs also. A correction factor compensating for this was determined by passing unlike-sign (US) pairs through the same

¹Contribution to the *Workshop on Particle Correlations and Femtoscopy*, Kroměříž, Czech Republic, 15–17 August 2005. To appear in: *Proc. 35th International Symposium on Multiparticle Dynamics*, Kroměříž, 9–15 August 2005, American Institute of Physics (2006).

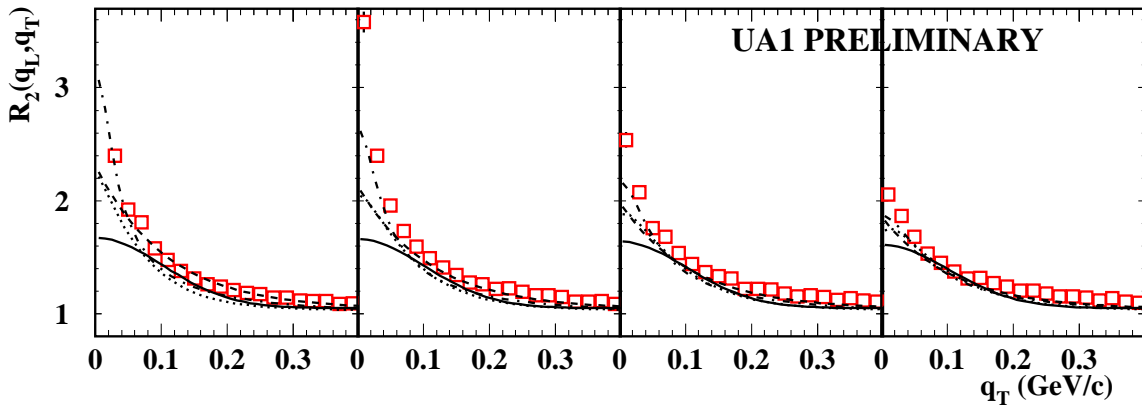
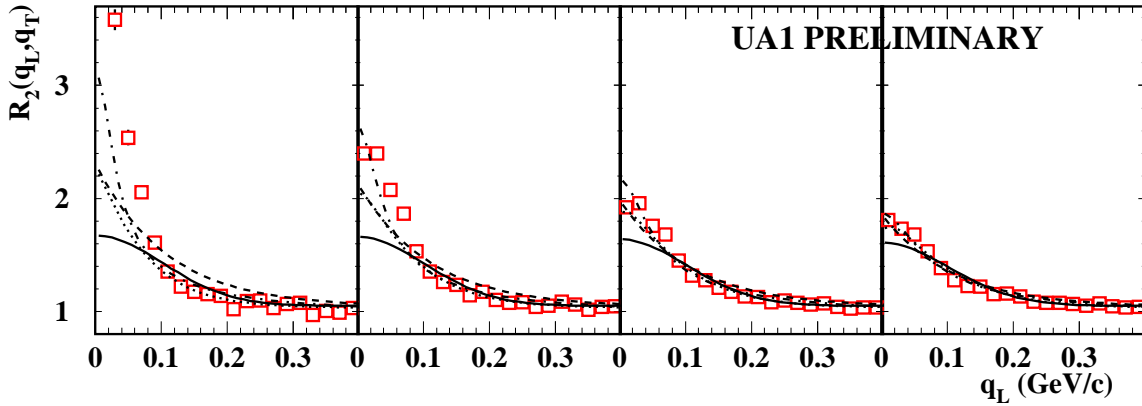
ghost-cut algorithm. Such correction factors were determined for each (q_L, q_T) bin² and charged-multiplicity subsample; for some (q_L, q_T) bins, this correction factor ranges up to 1.7 or even 1.9 for low-multiplicity subsamples.

We corrected for Coulomb repulsion by parametrising the Bowler Coulomb correction in the invariant momentum difference $Q = \sqrt{-(p_1 - p_2)^2}$ [5] with an exponentially damped Gamov factor $G(Q)$ [6], with a best-fit value $Q_{\text{eff}} = 0.173 \pm 0.001$ GeV/c,

$$F_{\text{coul}}(Q) = 1 + [G(Q) - 1] \exp(-Q/Q_{\text{eff}}). \quad (1)$$

The reference sample was formed by randomly combining LS tracks taken from pools of events in the same subsample of event charged multiplicity N as the sibling event currently being analysed. Note that the reference for fixed-multiplicity subsamples is not the poisson distribution but the multinomial, whose second moment is $\rho_2^{\text{mult}}(\mathbf{q}|N) = (1 - N^{-1})\rho_1 \otimes \rho_1(\mathbf{q}|N)$, so that the appropriate normalised moment is [1, 7]

$$R_2(\mathbf{q}) = \frac{\sum_N P_N \rho_2^{\text{LS}}(\mathbf{q}|N)}{\sum_N P_N (1 - N^{-1}) \rho_1 \otimes \rho_1^{\text{LS}}(\mathbf{q}|N)}. \quad (2)$$



²The (q_L, q_T) bins for ghost corrections use q_L measured in the detector rest system ($p\bar{p}$ CMS), while all HBT quantities are measured in the LCMS.

FIGURE 1. Upper panels: $R_2(q_L, q_T)$ data and best fits, shown for the first slices (left to right) $q_T = 0.00\text{--}0.02, 0.02\text{--}0.04, 0.04\text{--}0.06$ and $0.06\text{--}0.08$ GeV/c. Lower panels: $R_2(q_L, q_T)$ and the same fits for corresponding fixed- q_L slices. Solid lines: Gauss/Edgeworth fits; dashed: exponential; dotted: exponential with cross term; dash-dotted: Lévy. The bin $(q_L, q_T) < (0.02, 0.02)$ GeV/c is omitted from all fits and plots.

The ghost- and coulomb-corrected normalised moment $R_2(q_L, q_T)$ is shown in Fig. 1, together with fits to parametrisations $R_2 = \gamma[1 + \lambda|S_{12}|^2]$, with $|S_{12}|^2$ parametrised respectively as $\exp(-R_L^2 q_L^2 - R_T^2 q_T^2 - 2R_{LT} q_L q_T)$ (gauss with cross term), $\exp(-R_L q_L - R_T q_T)$ (exponential), $\exp(-R_L q_L - R_T q_T - 2R_{LT} \sqrt{q_L q_T})$ (exponential with cross term) and $R_2 = \gamma [1 + (R_L q_L)^{-\alpha_L} (R_T q_T)^{-\alpha_T}]$ (product power law). Note that all results shown are preliminary.

It is immediately apparent that none of these fits reproduces the data, with χ^2/NDF ranging from 3 to 9. A parametrisation based on an Edgeworth expansion [8, 9],

$$|S_{12}|^2 = \exp(-R_L^2 q_L^2 - R_T^2 q_T^2) \prod_{d=L,T} \left[1 + \kappa_{4,d} H_4(\sqrt{2} R_d q_d)/24 \right], \quad (3)$$

(with $\kappa_{4,d}$ the fourth-order cumulant in q_d and H_4 the corresponding hermite polynomial) fares no better as best-fit values for $\kappa_{4,d}$ in both directions turn out to be negligible. We omit the third-order terms in $\kappa_{3,L}$ and $\kappa_{3,T}$ as they are antisymmetric in q_d .

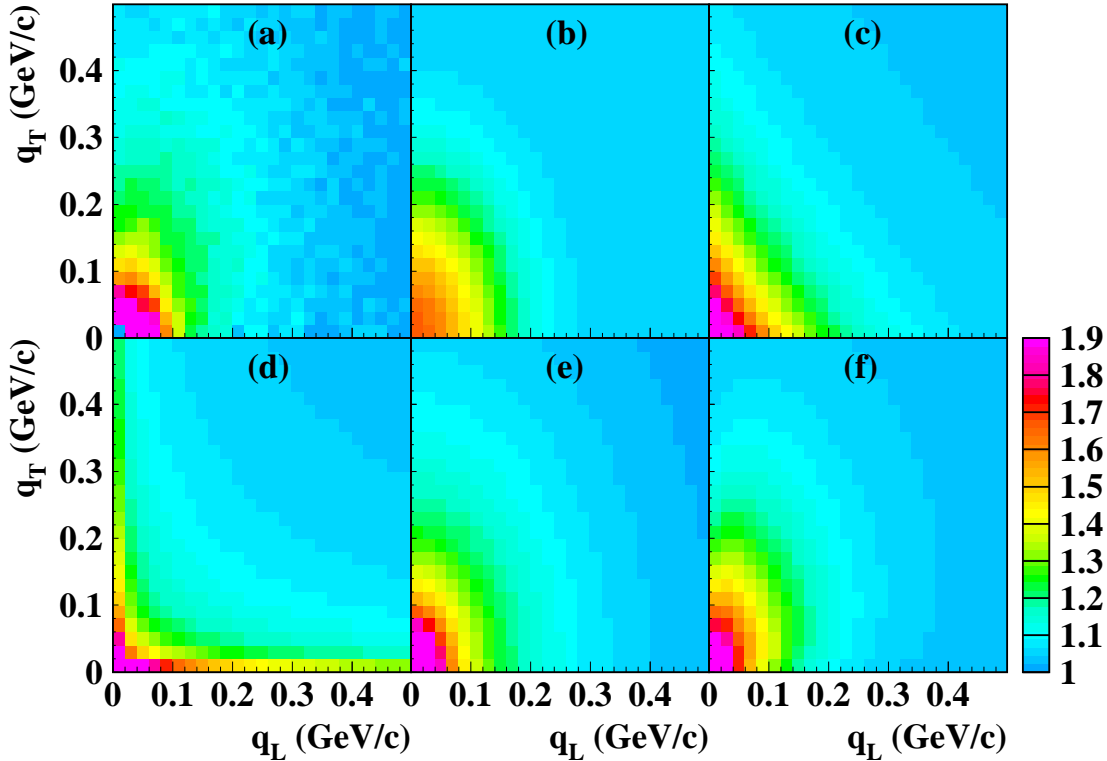


FIGURE 2: Comparing the shapes of $R_2(q_L, q_T)$ at intermediate scales. Panels show (a)) UA1 data, (b) gauss, (c) exponential, (d) power-law, (e) Lévy, (f) exponential with cross term fits. The gauss-type fits have the right shape, but end up far below the data peak

at small (q_L, q_T) . While the simple exponential and product power-law may approximate the peak reasonably, both fail miserably when shapes at intermediate scales are considered. Lévy does well but no unique best fit can be found. Shape-wise, the exponential with cross term (f) appears to come out on top. All plots are truncated at $R_2 \leq 1.9$ in order to bring out structure at intermediate scales.

A Lévy-based parametrisation [10],

$$|S_{12}|^2 = \exp(-R_L^2 q_L^2 - R_T^2 q_T^2)^{\alpha/2}, \quad (4)$$

yields better results in reproducing the strong peak observed in the data; however, four of the five fit parameters, viz. λ , R_L , R_T and α , are strongly correlated so that no unique best fit can be achieved. One example of many equivalent “best” fits is shown in Fig. 1. Omitting a second small- (q_L, q_T) bin from the Lévy fit renders the fit even more unstable (the innermost bin $(q_L, q_T) < (0.02, 0.02)$ GeV/c is excluded from all analysis as a matter of course). This is hardly surprising, as the four abovementioned parameters collectively depend strongly on the exact shape of the peak in the very small (q_L, q_T) region — the very region that experimental measurement struggles to resolve.

Interesting, nonetheless, is the observation that fits fail for different reasons: As shown in Fig. 2, the gauss and Edgeworth fits reproduce the shape of R_2 at intermediate (q_L, q_T) rather well but lacks the strong peak exhibited in the data,³ while the exponential and product power-law parametrisations are more peaked but fail to describe the shape at intermediate (q_L, q_T) . Judging by shape alone, the exponential with a $2R_{LT}\sqrt{q_L q_T}$ cross term does best (Fig. 2(f)).

Either way, it is clear that the superiority of the power-law fit to the one-dimensional invariant four-momentum moment $R_2(Q)$ over Gauss and exponential fits [4] is not repeated in the $R_2(q_L, q_T)$ case due to the hyperbolic shape of our “product power-law” parametrisation⁴ compared to the elliptic form of the $R_2(q_L, q_T)$ data shown in Fig. 2(a). The analysis of shapes at intermediate scales appears to provide valuable information. Shape analysis in the form of Refs. [11, 12] may help to quantify these qualitative observations.

The failure of conventional parametrisations to reproduce the elusive peak at small (q_L, q_T) suggests that there may be two scales in the system. Borrowing the (strictly speaking inappropriate) terms “core” and “halo” from the literature [13], we try a two-scale “butcher’s model”, similar to simpler precursors in Refs. [14, 15],

$$R_2(q_L, q_T) = \gamma \left[1 + \lambda_C \exp(-R_{LC}^2 q_L^2 - R_{TC}^2 q_T^2) + \lambda_H \exp(-R_{LH}^2 q_L^2 - R_{TH}^2 q_T^2) \right], \quad (5)$$

and proceed as follows: First, we fit only bins with momentum differences larger than a hard cutoff, $(q_L, q_T) > (q_{\text{cut}}, q_{\text{cut}})$, to the core gaussian. The resulting best-fit is subtracted from all data. The remaining halo “data” with $(q_L, q_T) \leq (q_{\text{cut}}, q_{\text{cut}})$ is then fit with the halo gaussian, and the resulting “core” and “halo” best fits combined. Data and fit histograms at various steps of this procedure are shown in Fig. 3.

³Edgeworth fits are indistinguishable from the normal gaussian fits throughout this analysis.

⁴Other forms, such as a “sum power law” $R_2 = \gamma [1 + (R_L q_L)^{-\alpha_L} + (R_T q_T)^{-\alpha_T}]$ remain to be tested.

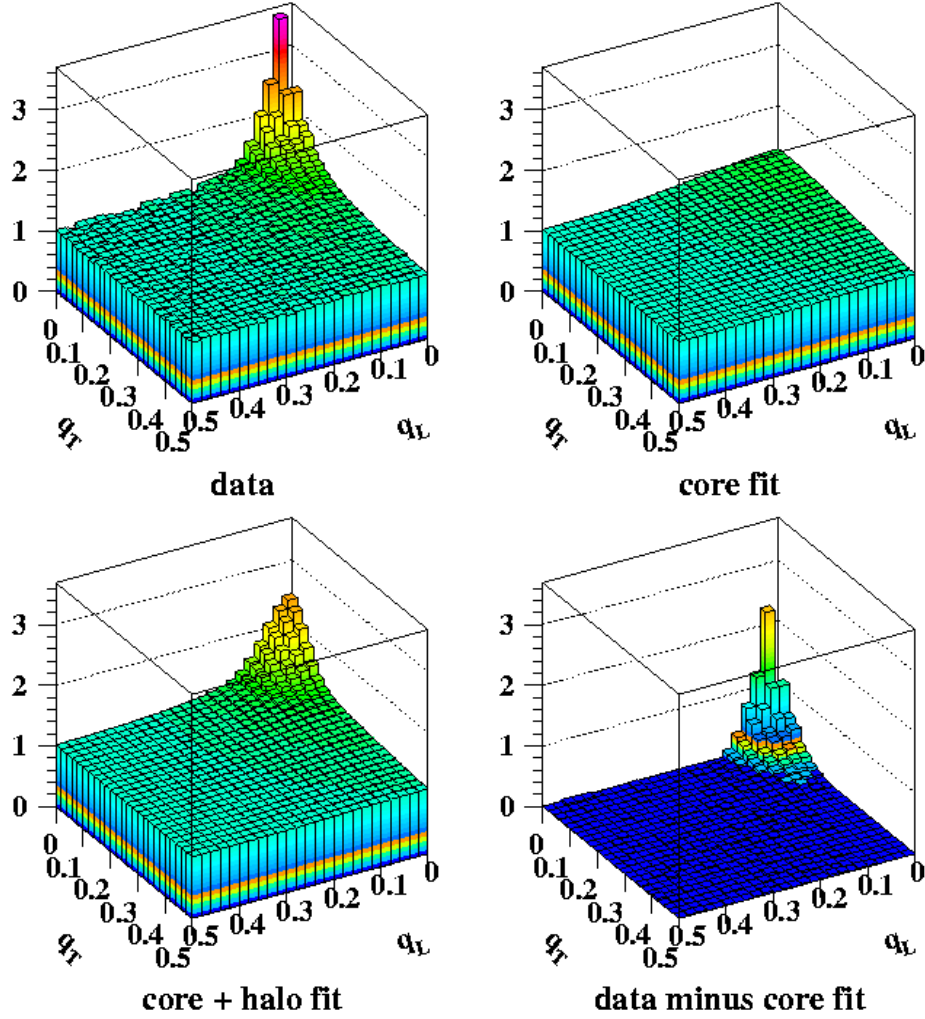


FIGURE 3: Two-scale butcher’s model. Of the $R_2(q_L, q_T)$ data (left upper panel) only bins with $(q_L, q_T) > (0.16, 0.16)$ GeV/c are fit to the “core” gaussian of Eq. (5) as shown in the right upper panel. The result is subtracted from the data to reveal the “halo” (right lower) which is then fit to the halo part of Eq. (5). The combined core-halo fit is shown in the left lower panel.

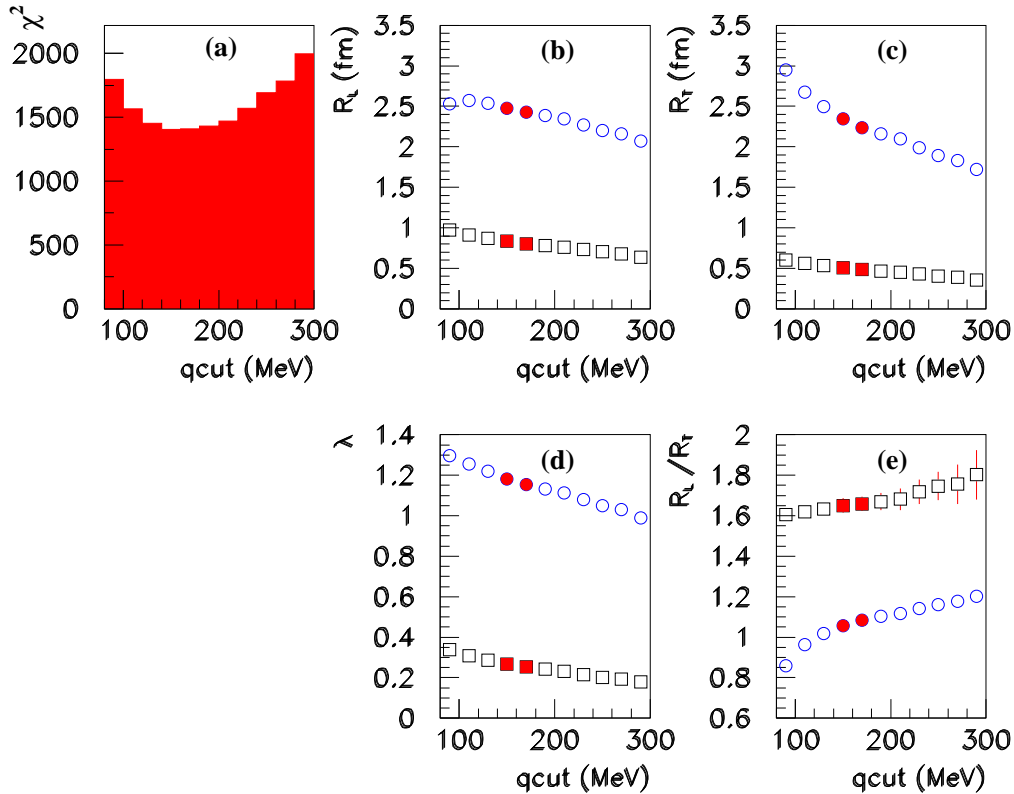


FIGURE 4: Dependence on q_{cut} . (a) Total χ^2 for both core and halo fits as a function of q_{cut} . The two lowest χ^2 values correspond to $q_{\text{cut}} = 0.16$ and 0.18 GeV/c, giving $\chi^2/\text{NDF} = 2.28$. Panels (b)–(e): Dependence of best-fit parameter values on q_{cut} . Squares and circles represent core and halo fit parameters respectively. A clear separation of scales is observed as assumed in the model. The halo continues to have a chaoticity parameter λ_H that exceeds its theoretical limit of 1.

In Fig. 4, the dependence of the two-scale model on q_{cut} is tested. As shown in Fig. 4(a), the joint χ^2 for both fits as a function of q_{cut} is found to have a well-defined minimum for $q_{\text{cut}} = 160\text{--}180$ MeV/c. The best estimates for R_L , R_T , λ and R_L/R_T are the two filled points in Fig. 4(b)–(e) corresponding to the two best q_{cut} values. Averaging these two numbers, we estimate $R_{LC} = 0.82 \pm 0.02$ fm, $R_{TC} = 0.49 \pm 0.02$ fm, $R_{LH} = 2.45 \pm 0.03$ fm, $R_{TH} = 2.29 \pm 0.05$ fm, $\lambda_C = 0.26 \pm 0.01$ and $\lambda_H = 1.17 \pm 0.02$, signalling a prolate “core” and a roughly spherical “halo”. The clear separation between the sizes of the core and halo radii *a posteriori* support the assumption of the presence of two scales, i.e. signal that the two-scale model is consistent. We note that λ_H continues to exceed the theoretical limit of 1.00, albeit not as strongly as the huge intercept $R_2(0,0) > 2.7$ seen in the data itself. *The joint best $\chi^2/\text{NDF} = 2.28$ for the two-scale model is still rather large, however, so that all numbers and conclusions should be treated with caution.*

Turning briefly to the more common three-dimensional Bertsch-Pratt representation [16], we find that the data once again has a strong peak at small (q_O, q_S, q_L) , and that the simple gaussian parametrisation fails completely. In Fig. 5, we show the result of fitting the Lévy and Edgeworth

parametrisations,

$$|S_{12}|^2 = \exp(-R_O^2 q_O^2 - R_S^2 q_S^2 - R_L^2 q_L^2)^{\alpha/2}, \quad (6)$$

$$|S_{12}|^2 = \exp(-R_O^2 q_O^2 - R_S^2 q_S^2 - R_L^2 q_L^2) \prod_{d=O,S,L} \left[1 + \kappa_{4,d} H_4(\sqrt{2} R_d q_d)/24 \right], \quad (7)$$

to $R_2(q_O, q_S, q_L)$, with slices plotted along the three axes of the three-dimensional space. Even these parametrisations appear not to describe the data well for small $|\mathbf{q}|$, and in this three-dimensional case the discrepancies are spread more widely than in the (q_L, q_T) case. Also, while the Lévy fit does appear to do reproduce the data to a reasonable degree, it again suffers from strong inherent correlations between the parameters λ, R_O, R_S, R_L and α . Such correlation again implies that no unique minimum for the χ^2 exists and thereby no unique best-fit values for its parameters either.

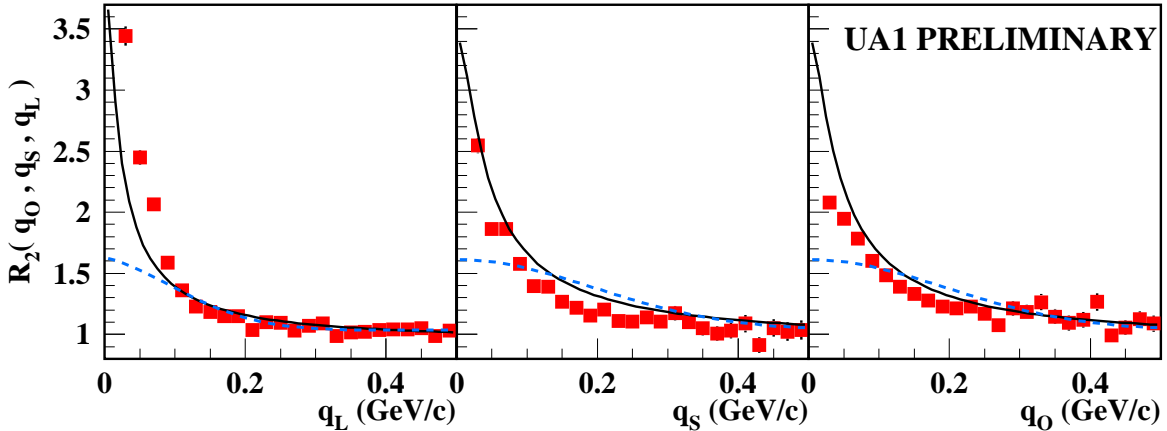


FIGURE 5: Second moment $R_2(q_O, q_S, q_L)$ of three-dimensional momentum difference decomposition, plotted along the three axes q_d , with the other two variables $(q_e, q_f) < (0.02, 0.02)$ GeV/c. Solid line: Lévy fit; dashed line: Edgeworth.

It is, of course, always possible to try even more elaborate parametrisations, for example using separate α -exponents for each of the (q_O, q_S, q_L) directions. While a better fit might theoretically be achieved, this will invariably come at the price of even more highly correlated parameters. The data cannot distinguish between many combinations of “best” values for such parameters.

We note that, even within the arguably artificial method of the two-scale model, the strong peak in the data is not reproduced, resulting in the quoted low confidence level. Nevertheless, it may provide a useful hint that “something else is going on”, be it the influence of jets, clustering effects or some other unknown factor.

We stress that it is unlikely that the strong peak seen in our data at small momentum differences, over and above simple gaussian or exponential parametrisations, is due to bias. First, the peak persists even without the Coulomb or split-track corrections. Second, we believe that the same peak may well be responsible for the power-law form and higher-order effects seen in our earlier work with one-dimensional distributions [4]. Third, the presence of unidentified kaons and protons in the sample imply that the real peak should exceed the one shown here, so that

the present results may be lower limits. It should also be noted that a number of other hadronic experiments have previously seen significant deviation from gaussian behaviour, especially at small $|\mathbf{q}|$ [17, 18]. The challenge is clearly now to find a convincing physical cause and explanation.

Acknowledgements: This work was supported in part by the National Research Foundation of South Africa. BB thanks the University of Stellenbosch for kind hospitality.

References

- [1] B. Buschbeck, H. C. Eggers and P. Lipa, *Phys. Lett.* **B481**, 187–193 (2000), hep-ex/0003029.
- [2] UA1 Collaboration; C. Albajar et al., *Phys. Lett.* **B226**, 410–416 (1989).
- [3] UA1 Collaboration, N. Neumeister et al., *Phys. Lett.* **B275**, 186 (1992).
- [4] H. C. Eggers, P. Lipa and B. Buschbeck, *Phys. Rev. Lett.* **79**, 197–200 (1997), hep-ph/9702235.
- [5] M.G. Bowler, *Phys. Lett.* **B270**, 69–74 (1991).
- [6] D. Brinkmann, PhD Thesis, University of Frankfurt (1995).
- [7] P. Lipa, H.C. Eggers and B. Buschbeck, *Phys. Rev.* **D53**, 4711–4714 (1996), hep-ph/9604373.
- [8] T. Csörgő, in: *Proc. Cracow Workshop on Multiparticle Production*, 1993, edited by A. Białas, K. Fiałkowski, K. Zalewski and R.C. Hwa, World Scientific (1994); pp. 175–186.
- [9] STAR Collaboration, J. Adams et al., nucl-ex/0411036.
- [10] T. Csörgő, S. Hegyi and W. A. Zajc, *Eur. Phys. J.* **C36**, 67–78 (2004), nucl-th/0310042.
- [11] P. Danielewicz and S. Pratt, *Phys. Lett.* **B618**, 60–67 (2005), nucl-th/0501003.
- [12] Z. Chajeccki, T.D. Gutierrez, M.A. Lisa and M. Lopez-Noriega (STAR Collaboration), in: *21st Winter Workshop on Nuclear Dynamics*, Breckenridge CO, February 2005, nucl-ex/0505009.
- [13] T. Csörgő, B. Lörstad and J. Zimányi, *Z. Phys.* **C71**, 491 (1994), hep-ph/9411307.
- [14] R. Lednitsky and M.I. Podgoretzkii, *Sov. J. Nucl. Phys.* **30**, 432 (1979);
R. Lednitsky et al., *Sov. J. Nucl. Phys.* **38**, 147 (1983).
- [15] EHS/NA22 Collaboration, N.M. Agababyan et al., *Z. Phys.* **C59**, 195–210 (1993).
- [16] G.F. Bertsch, M. Gong and M. Tohyama, *Phys. Rev.* **C37**, 1896–1900 (1988).
- [17] AFS Collaboration, T. Åkesson et al., *Phys. Lett.* **B129**, 269–272 (1983).
- [18] EHS/NA22 Collaboration, N. M. Agababyan et al., *Z. Phys.* **C68**, 229 (1995);
Z. Phys. **C71**, 405 (1996).